THE JOURNAL OF BIOLOGICAL CHEMISTRY Vol. 279, No. 48, Issue of November 26, pp. 50150–50156, 2004
© 2004 by The American Society for Biochemistry and Molecular Biology, Inc.
Printed in U.S.A.

Perturbation of Lipopolysaccharide (LPS) Micelles by Sushi 3 (S3) Antimicrobial Peptide

THE IMPORTANCE OF AN INTERMOLECULAR DISULFIDE BOND IN S3 DIMER FOR BINDING, DISRUPTION, AND NEUTRALIZATION OF LPS*

Received for publication, May 19, 2004, and in revised form, August 24, 2004
Published, JBC Papers in Press, August 24, 2004, DOI 10.1074/jbc.M405606200

Peng Li‡§, Thorsten Wohland¶, Bow Ho‖, and Jeak Ling Ding‡**

From the Departments of ‡Biological Sciences, ¶Chemistry, and ‖Microbiology, National University of Singapore, 117543 Singapore

S3 peptide, derived from the Sushi 3 domain of Factor C, which is the lipopolysaccharide (LPS)-sensitive serine protease of the horseshoe crab coagulation cascade, was shown previously to harbor antimicrobial activity against Gram-negative bacteria. However, the mechanism of action remains poorly understood at the molecular level. Here we demonstrate that the intermolecular disulfide bonding of S3 resulting in S3 dimers is indispensable for its interaction with LPS. The binding properties of the S3 monomer and dimer to LPS were analyzed by several approaches including enzyme-linked immunosorbent assay (ELISA)-based assay, surface plasmon resonance, and fluorescence correlation spectroscopy (FCS). It is evident that the S3 dimer exhibits stronger binding to LPS, demonstrating 50% LPS-neutralizing capability at a concentration of 1 μM. Circular dichroism spectrometry revealed that the S3 peptide undergoes conformational change in the presence of a disulfide bridge, transitioning from a random coil to β-sheet structure. Using a fluorescence correlation spectroscopy monitoring system, we describe a novel approach for examining the mechanism of peptide interaction with LPS in the native environment. The strategy shows that intermolecular disulfide bonding of S3 into dimers plays a critical role in its propensity to disrupt LPS micelles and consequently neutralize LPS activity. S3 dimers display detergent-like properties in disrupting LPS micelles. Considering intermolecular disulfide bonds as an important parameter in the structure-activity relationship, this insight provides clues for the future design of improved LPS-binding and -neutralizing peptides.

As a major constituent of the outer membrane of Gram-negative bacteria (GNB),[1] endotoxin or lipopolysaccharide (LPS) plays a key role in the pathophysiology of inflammation, sepsis, and shock (1). On release from the GNB, LPS interacts with the host plasma LPS-binding proteins. This interaction stimulates host monocytes and macrophages to secrete a wide array of inflammatory cytokines including tumor necrosis factor (2–4). Recent approaches to develop drugs to neutralize LPS have concentrated on characterizing the lipid A moiety of LPS using synthetic and recombinant peptides derived from sequences of polymyxin B sulfate, magainin, *Tachypleus* anti-LPS factor, recombinant limulus anti-LPS factor, bactericidal permeability-increasing protein, CAP-18, and lipopolysaccharide-binding protein (5, 6). These peptides are believed to induce complete lysis of the microorganism by perturbation or rupture of the membrane, which leads to leakage of bacterial cell components as well as dissipation of the electrical potential of the membrane (7). Such LPS-binding peptides are potentially active against microorganisms, despite being generally nontoxic to mammalian cells. The molecular basis for this selectivity and the underlying mechanism of permeation of GNB membranes remain ill defined but are believed to be related to the less negatively charged mammalian cell membranes (8, 9). To date, two hypotheses have been proposed for membrane perturbation, namely the "barrel-stave" and "carpet" mechanisms (10).

Diverse living organisms harbor arrays of innate immune molecules that contribute to the first line of defense against opportunistic pathogens (11). The horseshoe crab is dubbed a "living fossil," having survived virtually unchanged for ~400 million years of evolution. This is probably because of its strong innate immune system, which makes the organism highly resilient to threats from invading pathogens. LPS triggers a coagulation cascade in the horseshoe crab, which represents an important innate immune defense mechanism against the invading pathogen.

Being the initiator of the coagulation cascade, Factor C functions as a biosensor (12, 13) that responds to pg levels of LPS (14). Thus, it is conceivable that Factor C harbors an LPS binding motif(s) that exhibits exceptionally high affinity for LPS. The LPS binding domains of Factor C have been characterized (13, 15, 16). Near the N terminus of the multidomain Factor C molecule (17), there are several repeating units of Sushi domains of ~60 amino acids each. Sushi 1 and Sushi 3 contain LPS binding motifs. The core LPS binding

* This work was supported by the Agency for Science and Technology Research (A* STAR) of Singapore. The costs of publication of this article were defrayed in part by the payment of page charges. This article must therefore be hereby marked "*advertisement*" in accordance with 18 U.S.C. Section 1734 solely to indicate this fact.

§ Recipient of a Research Scholarship from the National University of Singapore.

** To whom correspondence should be addressed: Dept. of Biological Sciences, National University of Singapore, 14, Science Dr. 4, 117543 Singapore. Tel.: 65-6874-2776; Fax: 65-6779-2486; E-mail: dbsdjl@nus.edu.sg; World Wide Web: www.dbs.nus.edu.sg/Staff/ding.html.

[1] The abbreviations used are: GNB, Gram-negative bacteria; DTT, dithiothreitol; ELISA, enzyme-linked immunosorbent assay; ENC, endotoxin-neutralizing concentration; FCS, fluorescence correlation spectroscopy; FITC, fluorescein-5-isothiocyanate; LPS, lipopolysaccharide; N_F, number of fluorescent particles in the observation volume; PBS, phosphate-buffered saline; R_L, the ratio of large particles in solution; S3, Sushi 3 peptide; SPR, surface plasmon resonance; TMR, tetramethylrhodamine; Tricine, *N*-[2-hydroxy-1,1-bis(hydroxymethyl)ethyl]glycine; τ_D, the diffusion time; τ_{DS}, the diffusion time of the small particle; τ_{DL}, the diffusion time of the large particle; ABTS, 2,2′-azino-bis(3-ethylbenzthiazoline-6-sulfonic acid.

This paper is available on line at http://www.jbc.org

region of Sushi 3 resides in a 34-mer peptide, henceforth referred to as S3. Like most antimicrobial peptides, the mechanism of action of S3 is thought to be influenced by LPS (16). S3 has been demonstrated to bind and kill GNB (18). Because S3 peptide contains a single cysteine, it is conceivable that in solution, S3 exists in two forms, the monomeric peptide without a disulfide bond and the dimeric peptide linked by an intermolecular disulfide bond. It has been reported for some antimicrobial peptides that multimers are more active than their corresponding monomers (19–21). Thus, cysteine can affect the LPS binding ability of S3 peptides. To gain a global perspective on the tolerance of cysteine residues in S3 to amino acid substitutions, a mutant peptide named S3-C27S (where cysteine 27 was changed to serine, C27S) has been synthesized (Fig. 1*A*), and the structure-activity relationship was analyzed. The effects of the S–S bridged S3 and the conformationally altered mutant, S3-C27S, as well as their biological activities were investigated.

EXPERIMENTAL PROCEDURES

Materials—Lipid A from *Escherichia coli* strain F583, LPS from *E. coli* strain 0111:B4, and fluorescein-5-isothiocyanate (FITC)-LPS from *E. coli* strain 0111:B4 were purchased from Sigma. Tetramethylrhodamine (TMR) and FITC were obtained from Molecular Probes (Eugene, OR). PyroGene, a recombinant Factor C-based endotoxin detection kit, was acquired from Cambrex Inc. (East Rutherford, NJ). Pyrogen-free water for making buffers was from Baxter (Morton Grove, IL).

Peptides—Peptides used in this study were synthesized and purified by Genemed Synthesis Inc. (San Francisco, CA). The native S3 peptide, N-HAEHKVKIGVEQKYGQFPQGTEVTYTCSGNYFLM-C, with a molecular weight of 3,892, corresponds to residues 268–301 of the Factor C Sushi 3 domain (GenBank™/EBI accession number S77063). One mutation was made to substitute cysteine 27 for a serine residue, resulting in S3-C27S. S3-TMR is S3 peptide labeled with a fluorescent probe, TMR. All peptides, collectively referred to as Sushi peptides, were purified to >95% purity by high performance liquid chromatography. Unless otherwise stated, the peptide concentration in this assay refers to the monomeric form.

Molecular Weight Determination by Tris-Tricine Gel Electrophoresis—Peptides in reducing (with DTT) and non-reducing (without DTT) buffers were electrophoresed in 15% Tris-Tricine gel and detected by Coomassie Blue staining.

Detection of Secondary Structure by Circular Dichroism—CD spectra were recorded in phosphate buffer, pH 7. CD experiments were carried out using a Jasco J-810 CD spectropolarimeter. Spectra were recorded in quartz cell cuvettes of 10-mm path length. The parameters used were bandwidth = 2 nm, step resolution = 0.5 nm, response = 1 s, scan speed = 10 nm/min, and scan width = 190–260 nm. The temperature within the sample chamber was maintained at 25 °C with a continuous flow of nitrogen. Calibration was carried out with D-camphor sulfonic acid.

ELISA-based LPS Binding Assay—The polysorp 96-well plate (MaxiSorp™, Nunc) was first coated with 100 μl/well of 10 μg/ml (~1 μM) LPS from *E. coli* 0111:B4 in pyrogen-free phosphate-buffered saline (PBS). The plate was sealed and incubated overnight at room temperature. The wells were aspirated, washed four times with 300 μl of wash solution (PBS containing 0.05% Tween 20), and blocked with wash solution containing 2% bovine serum albumin at 37 °C for 3 h. After washing twice, increasing concentrations of peptides were allowed to interact with bound LPS at room temperature for 3 h. Bound peptides were detected by incubation with rabbit anti-S3 antibody followed by goat anti-rabbit antibody conjugated with horseradish peroxidase (Roche Applied Science). Each antibody was incubated for 2 h at 37 °C. In the final step, 100 μl of peroxide ABTS (2,2′-azino-bis(3-ethylbenzthiazoline-6-sulfonic acid) substrate was added. The absorbance was measured at 405 nm with a reference wavelength of 490 nm. The values were correlated to the amount of LPS bound and peptide present.

Surface Plasmon Resonance (SPR) Analysis of Real Time Interaction between S3 and Lipid A—The real time interaction between different concentrations of peptides and lipid A was performed according to Tan *et al.* (15) using biointeraction analysis (BIAcore 2000, Amersham Biosciences). The SPR was recorded on an HPA chip coated with *E. coli* F583 lipid A. The parameters used were flow rate of 20 μl/min, injection volume of 50 μl, and dissociation time of 180 s. The HPA chip was regenerated by a pulse of 0.1 N NaOH until the SPR reached the base line. The temperature within the sample chamber was maintained at 25 °C.

Fluorescence Correlation Spectroscopy (FCS)—The FCS instrument is a self-built system that is centered around a Zeiss Axiovert 200 inverted microscope (Carl Zeiss, Oberkochen, Germany) and uses an excitation source and argon-krypton laser (Melles Griot, Carlsbad, CA), which has a 488-nm line for fluorescein excitation and a 530-nm line for TMR excitation. The dichroic and emission filters (Omega Optical, Brattleboro, VT) were 570DRLP and 595AF60 for TMR and 505DRLP and 535DF35 for FITC. Further details on the FCS setup and theory are described in Wohland *et al.* (22) and Krichevsky *et al.* (23), respectively.

FCS provides three different parameters for our investigation. (i) One parameter is the diffusion coefficient of the different fluorescent species in the sample. The diffusion time, τ, is a measure of the average time a particle needs to traverse the confocal volume. The diffusion time is proportional to the cubic root of the mass. To distinguish two particles in solution, their diffusion times have to differ by a factor 1.6–2, meaning a 4–8-fold difference in mass (24, 25). (ii) A second parameter is the average total number of fluorescent particles, N_F, in the confocal volume, which is directly proportional to the concentration. (iii) Another parameter is the mole fraction of different particles comprising N_F when more than one type of particle is present. At any one time, not more than two different particles are present, and all measurements could be fitted with models assuming one or two particles in solution (22, 26). We therefore adopt the following convention. τ_{DS} is the diffusion time of the smaller particle. τ_{DL} is the diffusion time of the larger particle ($\tau_{DL} > \tau_{DS}$), and R_L is the mole fraction of the large particles in solution. The fraction of the smaller particles is therefore $1 - R_L$.

In Situ Monitoring of S3 Interaction with LPS Micelles by FCS—FCS was used to analyze the binding interaction between S3-TMR (M_r ~4,000) and LPS from *E. coli* 0111:B4 (M_r ~10,000; Ref. 27). Because of the closeness between the relative molecular weights of the two interacting components, the potential complexes of S3-TMR·LPS with a ratio ~1:2.5 cannot be detected by FCS. However, complexes of S3-TMR and large LPS micelles, which exist in solution (28), are detectable.

Measurements were conducted at a constant concentration of 50 nM S3-TMR and different concentrations of LPS (0–1 μM). The sample solutions were prepared at least 2 h before the measurements to ensure that binding equilibrium had been reached. A 50-μl droplet of the corresponding sample was then placed on a coverslip just before the measurement. The background signal in water and in the corresponding buffers was less than 0.2 kHz. All measurements were precalibrated with TMR and S3-TMR to ensure proper performance of the instrument. For each sample, at least 10 independent measurements were recorded.

To determine the effect of S3 on the LPS micelles, measurements were performed with unlabeled S3 on FITC-labeled LPS (FITC-LPS). Recordings were taken at an excitation wavelength of 488 nm, and calibrations were performed with FITC and FITC-LPS. In this case, the FITC-LPS concentration was fixed at 500 nM while different peptides were added, and the concentration of each peptide in solution was 10 μM. For sample preparation, the protocol described above was used. As control experiments, 0.2% Triton X-100, an LPS-active detergent known to be able to disrupt LPS (29), was added to the solution of FITC-LPS, and the interaction was monitored by FCS.

Endotoxin Neutralization Test—The recombinant Factor C (rFC) in the PyroGene kit is activated by LPS to catalyze the hydrolysis of a synthetic substrate to release a fluorescent product that is quantifiable at excitation and emission wavelengths of 380 and 440 nm, respectively. In this assay, Sushi peptides, which bind to LPS to inhibit its endotoxic activity, were incubated at different concentrations for 1 h at 37 °C with or without an equal volume of LPS in disposable, endotoxin-free borosilicate tubes. Fifty μl of each mixture was then dispensed into wells of a sterile microtiter plate (Nunclon™ surface, Nunc), followed by the addition of 50 μl of freshly reconstituted recombinant Factor C reagent. After 30 min, the fluorescence of each well was monitored at 440 nm, and the concentration of peptides corresponding to 50% inhibition of recombinant Factor C activity was designated ENC_{50}. Thus, the lower the ENC_{50} of the Sushi peptide, the greater is its ability to inhibit LPS.

RESULTS

The Native S3 Peptide Forms Dimers via Intermolecular Disulfide Bonds—Separation of peptides less than 10 kDa is not possible in the traditional discontinuous PAGE system. This is because of the co-migration of SDS and smaller proteins, which obscures the resolution. However, the Tris-Tricine

method that employs modified buffer conditions separates the peptides, thereby improving resolution. Fig. 1*B* shows that the molecular weights of the native S3 and mutant S3-C27S peptides in non-reducing buffer are about 8,000 and 4,000, respectively. In contrast, the molecular weights of the native S3 and mutant S3-C27S peptides in reducing buffer were about 4,000. This suggests that under physiological conditions, the native S3 peptides exist as dimers linked by intermolecular disulfide bonds. Furthermore, FCS measurements show that the number of fluorescent particles, N_F, was doubled (Fig. 1*C*) when DTT was added to a solution of 50 nM S3-TMR. This shows that the S–S bond between two S3 peptides was broken by DTT, which is responsible for the increase in the number of free fluorescent S3-TMR molecules in solution.

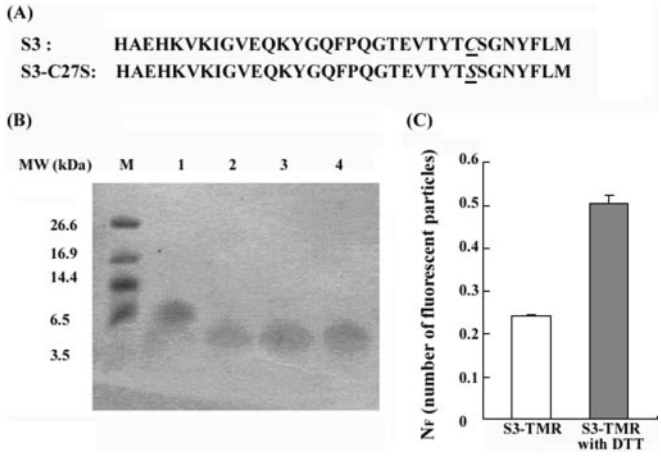

FIG. 1. **The native S3 peptide forms dimers via an intermolecular disulfide bond.** *A*, the amino acid sequences of the native and mutant S3 peptide. *B*, Tricine PAGE electrophoretic analysis of S3 and S3-C27S peptides under non-reducing and reducing conditions. *Lane M*, peptide molecular weight markers; *lane 1*, S3 (non-reducing); *lane 2*, S3 (reducing); *lane 3*, S3-C27S (non-reducing); *lane 4*, S3-C27S (reducing). *C*, experimental fluorescent particle number, N_F, for TMR-labeled S3 peptides in phosphate buffer, pH 7.4, with or without DTT.

Disulfide Bond Stabilizes S3—Upon addition of DTT, the CD spectrum of S3 changes significantly with the loss of negative peaks at 205 and 215 nm (Fig. 2). These two peaks most likely represent stable secondary structures such as α-helices and β-sheets. Moreover, the minimum ellipticity is above 200 nm. This increase in the absolute values of mean residue ellipticity may be because of fewer monomeric conformers in solution and the stabilization of the dimer. The calculated content of secondary structure elements suggests distinctive dimers of S3 with predominant antiparallel β-sheet conformation (36.8% β-sheet, 22.8% α-helix). In contrast, the S3-C27S mutant peptide adopts a random coil conformation in phosphate buffer, pH 7.0, with the single minimum ellipticity observed at 195–200 nm, which is close to the spectrum of the native S3 monomer (in DTT).

S3 Dimer Exhibits Higher Affinity for LPS Molecule—Anti-S3 antibody recognizes both S3 and S3-C27S peptides (Fig. 3*A*). The ELISA-based LPS binding assay revealed different binding capabilities between S3 and S3-C27S for LPS (Fig. 3*B*). Furthermore, at 2 μM, the S3 peptide reached saturation of binding to LPS, whereas the S3-C27S peptide continued linearly. Under these conditions, the native S3 is dimeric, whereas S3-C27S remains monomeric. This suggests that the S3 dimer has a higher affinity for LPS than the S3-C27S

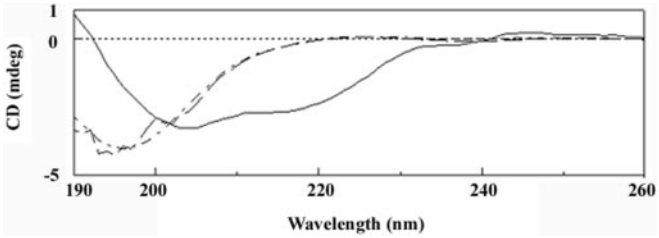

FIG. 2. **CD spectra of 10 μM S3 peptides in the presence of 10 mM phosphate buffer, pH 7.0 (PBS).** The conformational changes in the secondary structure of the native S3 monomer with DTT (– – –), native S3 dimer in buffer (——), and mutant S3-C27S (– · – ·) were recorded in buffer.

FIG. 3. **S3 dimer exhibits strong binding capacity for LPS.** *A*, ELISA using varying concentrations of native S3 peptide and mutant S3-C27S peptide coated on 96-well plates. The amount of bound peptides was determined by rabbit anti-S3 antibody and quantitated by ABTS substrate. The average of $A_{405\ nm}$ values of the triplicate samples was calculated and plotted with the corresponding concentrations of the peptides. *B*, ELISA-based LPS binding assay. LPS was coated overnight on 96-well plates. Varying concentrations of peptides were allowed to interact with the immobilized LPS. The amount of bound peptides was determined by rabbit anti-S3 antibody and quantitated by ABTS substrate. The average of $A_{405\ nm}$ values of the triplicate samples was calculated and plotted with the corresponding concentrations of peptides. *C*, the sensorgram depicting the real time interaction between Sushi peptides and the immobilized lipid A. Fifty μl of 5 μM peptides was injected, resulting in a sustained increase in the relative response units (RU). During the dissociation phase, pyrogen-free buffer was introduced at a flow rate of 20 μl/min. The HPA chip surface was regenerated by a pulse of 100 mM NaOH.

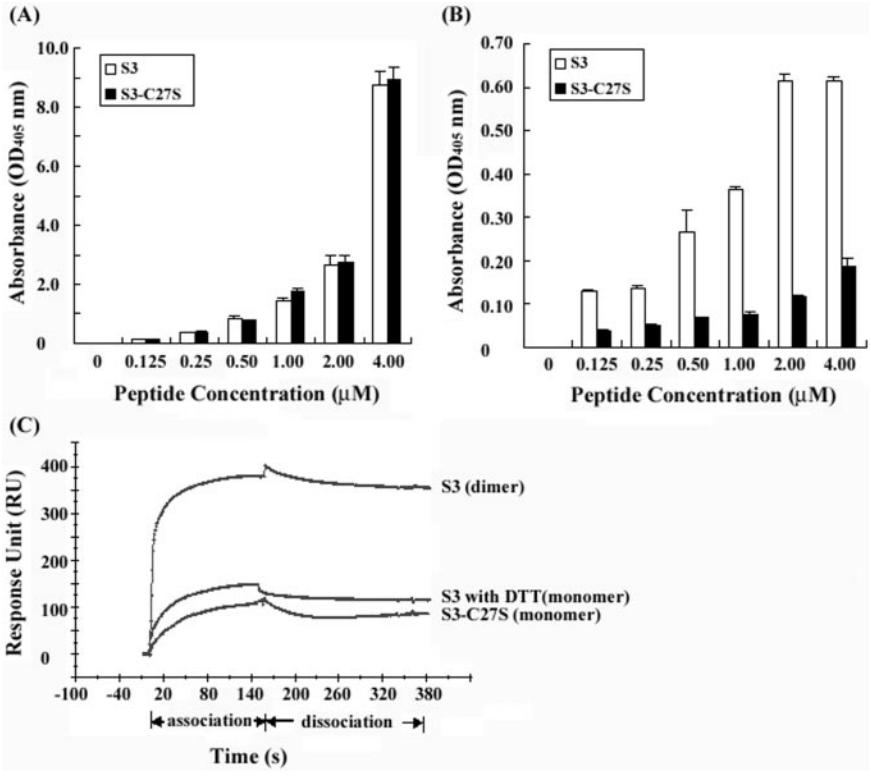

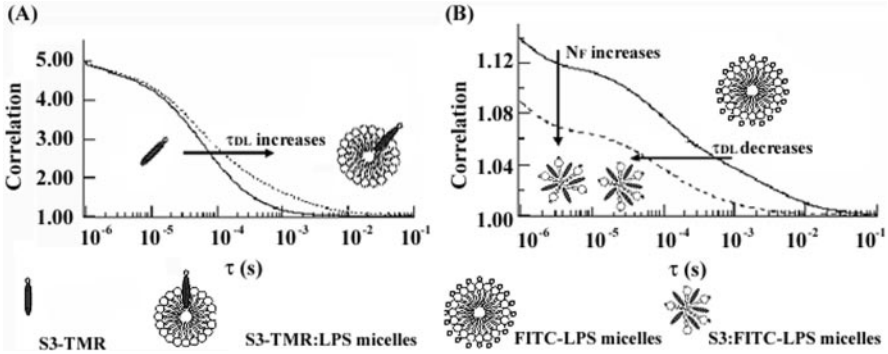

FIG. 4. **The autocorrelation curves of two FCS detection systems.** *A*, change in the diffusion time of a small S3 peptide as it interacts the large LPS micelles. When only S3-TMR exists in solution, the τ_{DL} of the particle was 8.99×10^{-5} s; upon addition of LPS micelles, τ_{DL} increased to $2.54 \times 10^{\times 3}$ s. This implies that S3-TMR binds larger LPS micelles, which slows down its diffusion as reflected by the increase in τ_{DL}. The autocorrelation curves of S3-TMR and S3-TMR·LPS micelles are shown by *solid* and *broken lines*, respectively. *B*, interaction with increasing concentrations of S3 peptide caused a decrease in the diffusion time (τ_{DL}) of the complex as the large FITC-LPS micelle was disrupted into small S3·FITC-LPS micelles. As an example, when only the FITC-LPS micelle was present in solution, the τ_{DL} of the particle is 3.31×10^{-3} s, and the N_F of the fluorescence particle is 5.48. In contrast, after S3 peptide interacted with the FITC-LPS micelle to disrupt the micellar complex, the τ_{DL} decreased to 1.21×10^{-3} s, and the N_F of S3·FITC-LPS micelles increased to 7.81, resulting in smaller S3·FITC-LPS micelles. This result shows that FITC-LPS micelles are disrupted by S3 dimer peptide, which increases the diffusion time as reflected by a decrease in τ_{DL}. The autocorrelation curves of the larger FITC-LPS micelles and the smaller S3·FITC-LPS micelles are annotated by *solid* and *broken lines*, respectively.

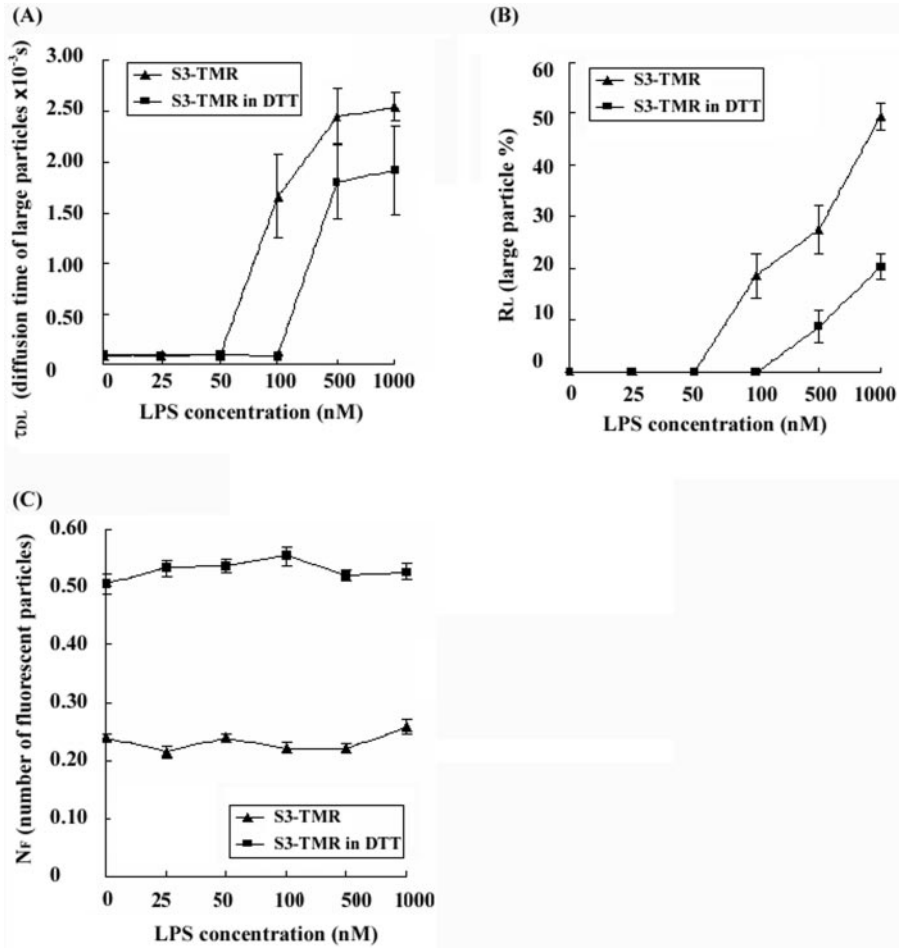

FIG. 5. **Determination of the stoichiometry of interaction between LPS and S3-TMR.** The concentration of fluorescent particles/complexes was measured for reaction mixtures containing S3-TMR and increasing concentrations of LPS. The S3-TMR was held constant at 50 nM. For S3 dimer (▲) or S3 in DTT (■), the concentrations increased from 0 to 1 μM. *A*, compared with S3 monomer, the S3 dimer caused a more rapid increase in τ_{DL}, which is the number of large particles in solution. *B*, R_L, which is the ratio of large particles, increased more rapidly with S3 dimer than with S3 monomer. *C*, N_F of S3 monomer is 2× greater than that of S3 dimer. All data points are averaged over 10 experiments.

monomer. The real time binding analysis shows that the interaction between S3 and lipid A reached equilibrium during the injection of the sample. To compare the affinity of several Sushi peptides for *E. coli* lipid A, different kinds of peptides at the same concentration in buffer were injected across a lipid A-coated HPA chip. The sensorgrams revealed that the SPR signal intensity increased as a function of the concentration of the peptide bound to the immobilized lipid A (Fig. 3*C*). This indicates that the amount of peptide bound to lipid A is related to the affinity of the peptide for lipid A on the chip. At the same concentration, S3 dimer achieved 2-fold higher response units than the S3-C27S or S3 monomer, viz, S3 treated with DTT (Fig. 3*C*). The affinity of S3 dimer to negatively charged lipid A is higher than S3 monomer, similar to what has been obtained by ELISA. To exclude the possibility of the direct effect of DTT on the SPR signals, the binding interaction between S3-C27S in DTT and lipid A was performed. No significant change in affinity was observed between S3-C27S alone and S3-C27S in

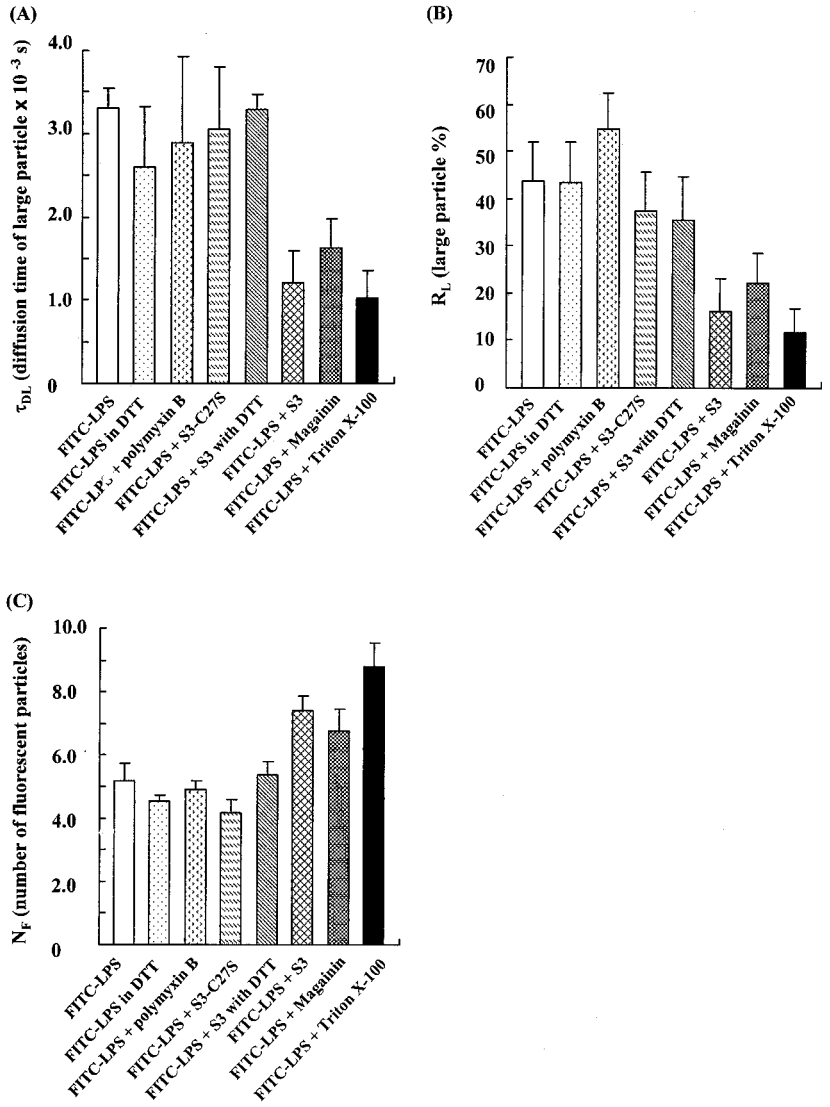

FIG. 6. **Determination of the stoichiometry of FITC-LPS micelles and peptide interaction.** The concentration of fluorescent particles was measured for samples of FITC-LPS under different conditions. The FITC-LPS was held constant at 500 nM. The concentrations of peptide and Triton X-100 were 10 μM and 0.2%, respectively. *A*, in a control experiment with FITC-LPS alone and FITC-LPS in 5 mM DTT, the τ_{DL} values were 3.31×10^{-3} and 2.59×10^{-3}, respectively. In the case of S3 dimer, the τ_{DL} decreased to 1.21×10^{-3}. The interaction between FITC-LPS and magainin or FITC-LPS and Triton X-100 exhibited a similar trend of decreasing τ_{DL}. This indicates that all three above mentioned LPS-active agents (S3 dimer, magainin, and Triton X-100) caused the reduction of the diameter of fluorescent particles of FITC-LPS. This is analogous to the perturbation of the LPS micelles. In contrast, interaction between FITC-LPS and the same concentrations of S3-C27S and S3 (in DTT) did not change τ_{DL} significantly. *B*, in a control experiment with FITC-LPS and FITC-LPS in 5 mM DTT, the R_L values were 43.69 and 43.41%, respectively. In the presence of S3 dimer, the R_L of FITC-LPS decreased to 16.22%. This is similar to FITC-LPS in magainin and to FITC-LPS in Triton X-100. This represents the disruption of FITC-LPS micelles, resulting in the release of small fluorescent particles such as free FITC-LPS molecules. *C*, in contrast, N_F did not change significantly during interactions between FITC-LPS and the same concentrations of S3-C27S and S3 in DTT, where the N_F values were 5.18 and 4.56, respectively. In the presence of S3 dimer, the N_F increased to 7.41. Magainin and Triton X-100 effected a similar increase in N_F values. All data points are averaged over 10 experiments.

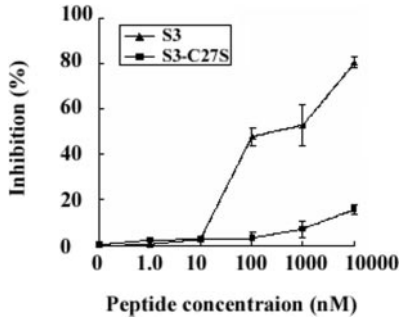

FIG. 7. **Inhibition of the LPS-induced recombinant Factor C in the PyroGene assay.** Binding of the peptides to LPS competitively inhibits the LPS-induced recombinant Factor C activity. Compared with S3-C27S, S3 dimer shows superior ability to inhibit LPS activity.

DTT. This indicates that intermolecular disulfide bonding plays a key role in the formation of the S3 dimer, which contributes to its elevated affinity for endotoxin.

FCS Shows That the Native S3 Dimer Binds Avidly to and Disrupts LPS Micelles in Solution—Molecular interactions between two different molecules (LPS and S3 peptide) can be monitored by the diffusion time (τ_{DL}), the concentration of fluorescent particles (N_F), and the fraction of bound complexes (R_L). In both FCS experiments, one of two interacting components was labeled by a fluorescent dye, viz, either S3-TMR (Fig. 4*A*) or FITC-LPS (Fig. 4*B*). Upon binding of a small labeled peptide like S3-TMR to a large LPS micelle, the change in diffusion time is readily detected. In the absence of LPS micelles, only one diffusion time is detected (τ = 90 μs), representing the value of unbound freely diffusing S3-TMR. In the presence of LPS, the S3-TMR binds LPS micelles showing an increase in the average diffusion time of the sample (Fig. 4*A*). Proper fits are obtained only when assuming at least two different particles in solution, unbound S3-TMR (or small S3-TMR·LPS oligomeric complexes that are not sufficiently different in mass to be detected) and S3-TMR·LPS micellar complexes. The change in the LPS micelles during the interaction between FITC-LPS and S3 dimer is reflected by a decrease in τ_{DL} with a concomitant increase in the particle number, N_F (Fig. 4*B*), during which the S3 peptide binds to FITC-LPS micelles to disrupt their micellar structure.

Fig. 5 compares the binding relationship between S3-TMR and LPS, showing that S3-TMR dimer has stronger affinity for LPS than S3-TMR monomer. This result is consistent with those obtained from ELISA and SPR analyses. Thus, at the initial low concentrations of S3-TMR, the free form of S3-TMR is the predominant fluorescent species. During the course of the interaction, the percentage of the complex continuously increases as the ligand concentration is increased, as demonstrated by the increase in R_L. A concomitant increase of τ_{DL} shows that with increasing LPS concentrations, larger LPS micelles are formed.

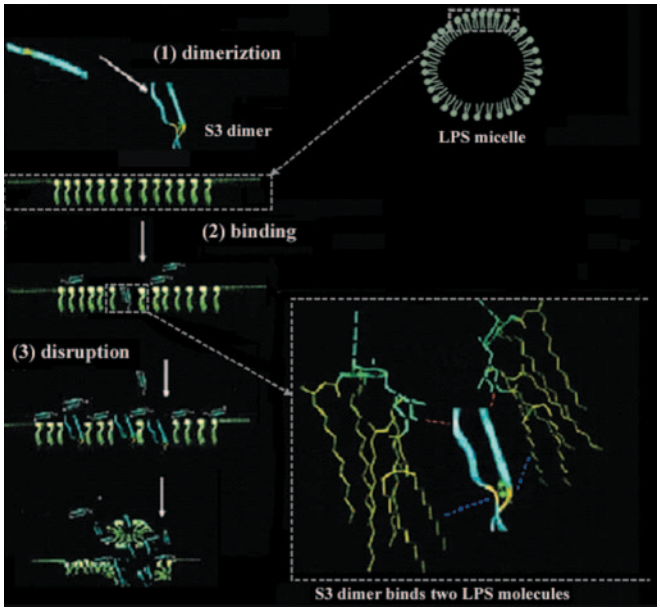

FIG. 8. **A hypothetical model for the mechanism of S3 dimer-mediated perturbation of LPS.** *1*, dimerization of S3 peptide occurs through an intermolecular disulfide bond. *2*, at the initial low ratio of S3:LPS, binding of S3 dimer to LPS occurs via (*a*) electrostatic interactions between the positively charged amino acid residues near the N termini of S3 dimer and the negatively charged bisphosphate head groups of the lipid A moiety of LPS and (*b*) hydrophobic interactions between the C termini of S3 dimer and the acyl chains of lipid A. This molecular interaction is stabilized through disulfide bonding of S3 dimer (*inset*). *3*, as the concentration of S3 dimer increases, the hydrophobic insertion of the peptide into the LPS layer results in pore formation, which is maintained by multiple points of chemical interaction between one S3 dimer and two LPS molecules, forming a trio complex of LPS·S3 dimer·LPS (*inset*). This initiates the disruption of LPS micelles. When a threshold concentration of S3 dimer peptide is reached, the perturbation of LPS is maximal.

This propensity of LPS to form larger micelles at higher concentrations was reported in literature (27).

To investigate the change in LPS micelles in the presence of S3, FITC-LPS was used in FCS experiments. A two-component fitting model was employed. The small component is free FITC-LPS (including FITC-LPS·S3 complexes), whereas the large component represents FITC-LPS micelles (including FITC-LPS micelle·S3 complexes). In the absence of S3, large fluorescent FITC-LPS micelles were present. During the interaction, the τ_{DS} is kept constant at 9.8×10^{-5} s, whereas the τ_{DL} and R_L progressively decrease as the concentration of S3 peptide is increased; this indicates that the S3 dimer interacts with and perturbs the large LPS micelles while N_F increases. S3 dimers rather than S3 monomers resulted in fewer LPS micelles (Fig. 6). In comparison with S3, high concentrations of magainin decreased τ_{DL} and R_L and increased the particle number N_F, which suggests that magainin can also disrupt LPS micelles. On the other hand, S3-C27S and S3 monomer did not cause significant change in R_L or τ_{DL}, and N_F remained constant (Fig. 6, *A–C*), suggesting that the S3 monomer is incapable of disrupting the LPS micelles even at high concentrations.

As a system control for FCS measurements, it was shown that Triton X-100 interactions with LPS micelles differ from those of the S3 monomer (Fig. 6). Like the S3 dimer, 0.2% Triton X-100 interacts with FITC-LPS to decrease τ_{DL} and R_L and to increase N_F. The disruption of LPS micelles by Triton X-100 demonstrates the *bona fide* observation of disruption of LPS micelles seen under FCS, thus authenticating the ability of S3 dimer to disrupt LPS micelles.

The Native S3 Dimer Inhibits LPS-induced Recombinant Factor C Activity—To examine the biological functionality of S3 peptides, a sensitive and precise fluorometric assay was used to assess the ability of native S3 and S3-C27S peptides to bind 50 enzyme units (EU)/ml endotoxin. Compared with the mutant S3-C27S peptide, which exists as a monomer, the native dimeric S3 peptide causes 10-fold greater inhibition of the LPS-induced recombinant Factor C activity (Fig. 7). A low ENC_{50} is indicative of the high potency of the peptide to neutralize LPS, with concomitant inhibition of the LPS-induced Factor C activity. The ENC_{50} values of the two peptides were determined to be 1 μM for S3 and >10 μM for S3-C27S.

DISCUSSION

The Dimeric Rather than the Monomeric Form of S3 Displays Strong LPS-binding and -neutralizing Activity—As shown by Tricine PAGE and FCS, the native S3 peptides have a propensity to dimerize via an intermolecular disulfide bond (Fig. 1, *B* and *C*), which is responsible for its high affinity for LPS. The disulfide bond stabilizes the secondary structure of the S3 dimer (Fig. 2), in agreement with the report of Tam *et al.* (30). Presumably, this structure is important for the interaction between S3 dimer and LPS, during which the S3 dimer forms a β-sheet structure to provide better shielding of the hydrophobic acyl chains of LPS (31). This may explain why the S3 dimer displays a stronger LPS-neutralizing capability than its monomeric counterpart. This possibility is clearly demonstrated and corroborated by the S3-C27S mutant, which as a monomer exhibits a complete structural changeover with a marked decrease in binding and a lack of suppression of LPS-induced toxicity.

The strong affinity of S3 dimer for LPS is confirmed by a panel of experiments including SPR, ELISA, and FCS. SPR and ELISA are surface-based techniques, which may not represent the absolute interactive behavior of two molecular components in solution. However, it is consistently evident from all three experimental approaches that the S3 dimer, stabilized by intermolecular disulfide bonding, exhibits a higher affinity for LPS (Fig. 3, *B* and *C*). Using FCS, we compared the activity of the peptides in solution. During titrations of S3-TMR with LPS, the dimer consistently showed stronger binding than the monomer as indicated by the larger fraction of R_L and longer diffusion time (τ_{DL}) of peptides bound to LPS micelles at all concentrations. Furthermore, the FITC-LPS system revealed a decrease in τ_{DL} with an accompanying increase in the particle number N_F, indicating that S3 dimers rather than their monomeric counterparts had disrupted the LPS micelles (Fig. 4).

S3 Dimer Disrupts LPS Micelles via a "Detergent-like" Mechanism—By FCS analysis, S3 dimer and Triton X-100 apparently exhibited the same specific activities for LPS micelles (Fig. 6). S3 peptide was shown to attain a detergent-like activity after reaching a threshold concentration. This is consistent with the report by Bechinger (32). Triton X-100 can be employed in two-phase LPS extraction. Above the critical micellar concentration of Triton X-100, LPS micelles are disrupted by non-polar interactions between the alkyl chains of LPS and Triton X-100 and are consequently separated from the water phase (33). In a similar manner, it is possible that at high concentrations S3 dimer binds the acyl chains of LPS, thereby disrupting the critical force that maintains the stability of the LPS micelles. Besides hydrophobic interactions, it is important to consider the electrostatic forces between the peptide and LPS in aqueous solutions (34–36). Near the N terminus of S3 there are several positively charged amino acids such as lysine residues, whereas the C terminus of S3 is more hydrophobic. The diphosphoryl head groups on the LPS confer a net negative charge, whereas its acyl chains are hydrophobic. S3 binds LPS through a preliminary interaction between the cationic amino acids at the N terminus of S3 and the diphosphoryl head groups of LPS, followed by stabilization of the resulting molecular

complex through a hydrophobic interaction via the C terminus of S3 and fatty acyl chains of LPS (Fig. 8). This is in agreement with our previous observation that mutations of the N terminus to introduce two extra lysine residues into S3 resulted in an increase in LPS-neutralizing activity (16). Considering the recent report that the aggregated form of LPS is biologically more active than the free LPS molecules (37), disruption of the LPS micelles by S3 dimer peptides may be related to LPS neutralization.

A Hypothetical Model for Peptide-LPS Interaction—Fig. 8 illustrates our proposed hypothetical model, which indicates that the dimeric form of S3 interacts preferentially with LPS molecules. This model may be summarized as follows. 1) Dimerization of S3 peptide occurs through an intermolecular disulfide bond. 2) At the initial low ratio of S3:LPS, binding of the S3 dimer to LPS micelle occurs via electrostatic and hydrophobic interactions. 3) As more S3 dimer accumulates at the local environment of the LPS micelle, the insertion of the peptide into the LPS layer initiates its disruption. When a threshold concentration of S3 dimer peptide is reached, perturbation of the LPS micelle is maximal, culminating in pore formation and complete disruption of the LPS layer. In contrast to the random S3 monomer peptide, which has weaker activity against LPS (Fig. 6), the S3 dimer is a symmetrically structured peptide. Therefore, we propose that in the interaction process, one S3 dimer binds two LPS molecules to form a complex constituting a trio of LPS·S3 dimer·LPS (Fig. 8, *inset*).

In conclusion, we have documented the use of fluorescence correlation spectroscopy as a novel solution-based approach to monitor the molecular interaction between the S3 dimer peptide and LPS. In consideration with several other surface-based biochemical approaches, we demonstrate the critical role of the intermolecular disulfide bond in the dimeric S3 peptide, which displays detergent-like properties to bind avidly to LPS, equipping the S3 dimer to preferentially disrupt the LPS micelles. This activity is related to the β-sheet secondary structure, which confers stability to the S3 dimer for its prolonged and persistent interaction with and disruption of LPS micelles. The significance of the intermolecular disulfide bond to the activity of an antiendotoxin peptide suggests new ways to improve the future design of LPS-neutralizing peptides.

REFERENCES

1. Breithaupt, H. (1999) *Nat. Biotechnol.* **17,** 1165–1169
2. Yazawa, N., Fujimoto, M., Sato, S., Miyake, K., Asano, N., Nagai, Y., Takeuchi, O., Takeda, K., Okochi, H., Akira, S., Tedder, T. F., and Tamaki, K. (2003) *Blood* **102,** 1374–1380
3. Kaksonen, M., Sun, Y., and Drubin, D. G. (2003) *Cell* **115,** 475–487
4. Gee, K., Kozlowski, M., and Kumar, A. (2003) *J. Biol. Chem.* **278,** 37275–37287
5. Epand, R. M., and Vogel, H. J. (1999) *Biochim. Biophys. Acta* **1462,** 11–28
6. Thomas, C. J., Surolia, N., and Surolia, A. (2001) *J. Biol. Chem.* **276,** 35701–35706
7. Nizet, V., Ohtake, T., Lauth, X., Trowbridge, J., Rudisill, J., Dorschner, R. A., Pestonjamasp, V., Piraino, J., Huttner, K., and Gallo, R. L. (2001) *Nature* **414,** 454–457
8. Gidalevita, D., Ishitsuka, Y., Muresan, A. S., Konovalov, O., Waring, A. J., Lehrer, R. I., Lee, K. Y. (2003) *Proc. Natl. Acad. Sci. U. S. A.* **100,** 6302–6307
9. Feder, R., Dagan, A., and Mor, A. (2000) *J. Biol. Chem.* **275,** 4230–4238
10. Oren, Z., Hong, J., and Shai, Y. (1997) *J. Biol. Chem.* **272,** 14643–14649
11. Zasloff, M. (2002) *Nature* **415,** 389–395
12. Ding, J. L., Navas, M. A., III, and Ho, B. (1993) *Biochim. Biophys. Acta* **1202,** 149–156
13. Ding, J. L., Navas, M. A., III, and Ho, B. (1995) *Mol. Mar. Biol. Biotechnol.* **4,** 90–103
14. Ho, B. (1983) *Microbios. Lett.* **24,** 81–84
15. Tan, N. S., Ho, B., and Ding, J. L. (2000) *FASEB J.* **14,** 859–870
16. Tan, N. S., Ng, M. L., Yau, Y. H., Chong, P. K., Ho, B., and Ding, J. L. (2000) *FASEB J.* **14,** 1801–1813
17. Wang, J., Tan, N. S., Ho, B., and Ding, J. L. (2002) *J. Biol. Chem.* **277,** 36363–36372
18. Yau, Y. H., Ho, B., Tan, N. S., Ng, M. L., and Ding, J. L. (2001) *Antimicrob. Agents Chemother.* **45,** 2820–2825
19. Lai, J. R., Huck, B. R., Weisblum, B., and Gellman, S. H. (2002) *Biochemistry* **41,** 12835–12842
20. Situ, H., Wei, G., Smith, C. J., Mashhoon, S., and Bobek, L. A. (2003) *Biochem. J.* **375,** 175–182
21. Wu, Z., Hoover, D. M., Yang, D., Boulegue, C., Santamaria, F., Oppenheim, J. J., Lubkowski, J., and Lu, W. (2003) *Proc. Natl. Acad. Sci. U. S. A.* **100,** 8880–8885
22. Wohland, T., Friedrich, K., Hovius, R., and Vogel, H. (1999) *Biochemistry* **38,** 8671–8681
23. Krichevsky, O., and Bonnet, G. (2002) *Rep. Prog. Phys.* **65,** 251–297
24. Wohland, T., Rigler, R., and Vogel, H. (2001) *Biophys. J.* **80,** 2987–2999
25. Meseth, U., Wohland, T., Rigler, R., and Vogel, H. (1999) *Biophys. J.* **76,** 1619–1631
26. Wohland, T., Friedrich, K., and Pick, H. (2001) in *Nobel Conference Lectures* (Rigler, R., Orrit, M., and Basché, T., eds) pp. 195–210, Springer-Verlag, Berlin
27. Aurell, C. A., and Wistrom, A. O. (1998) *Biochem. Biophys. Res. Commun.* **253,** 119–123
28. Neumann, L., Wohland, T., Whelan, R. J., Zare, R. N., and Kobilka, B. K. (2002) *Chembiochem.* **3,** 993–998
29. Petsch, D., and Anspach, F. B. (2000) *J. Biotechnol.* **76,** 97–119
30. Tam, J. P., Lu, Y. A., and Yang, J. L. (2002) *J. Biol. Chem.* **277,** 50450–50456
31. Ferguson, A. D., Hofmann, E., and Coulton, J. W. (1998) *Science* **282,** 2215–2220
32. Bechinger, B. (1997) *J. Membr. Biol.* **156,** 197–211
33. Bordier, C. (1981) *J. Biol. Chem.* **256**, 1604–1607
34. Frecer, V., Ho, B., and Ding, J. L. (2000) *Biochim. Biophys. Acta* **1466,** 87–104
35. Frecer, V., Ho, B., and Ding, J. L. (2000) *Eur. J. Biochem.* **267,** 837–852
36. Ding, J. L., Zhu, Y., and Ho, B. (2001) *J. Chromatogr. B Biomed. Sci. Appl.* **759,** 237–246
37. Mueller, M., Lindner, B., Kusumoto, S., Fukase, K., Schromm, A. B., and Seydel, U. (2004) *J. Biol. Chem.* **279,** 26307–26313